Study of the formation process and the characteristics of tantalum layers electrodeposited on Nitinol plates in the 1-butyl-1-methylpyrrolidinium bis(trifluoromethylsulfonyl)imide ionic liquid

Maho, A.; Delhalle, J.; Mekhalif, Z.

Published in:
Electrochimica Acta

DOI:
10.1016/j.electacta.2012.11.026

Publication date:
2013

Document Version
Peer reviewed version

Study of the formation process and the characteristics of tantalum layers electrodeposited on Nitinol plates in the 1-butyl-1-methylpyrrolidinium bis(trifluoromethylsulfonyl)imide ionic liquid

A. Maho[a, b], J. Delhalle[a], Z. Mekhalif[a,*]

[a] Laboratory of Chemistry and Electrochemistry of Surfaces, Facultés Universitaires Notre-Dame de la Paix (FUNDP), Rue de Bruxelles 61, B-5000 Namur, Belgium. E-mail: zineb.mekhalif@fundp.ac.be

[b] Fonds pour la Formation à la Recherche dans l'Industrie et dans l'Agriculture (FRIA), Rue d'Egmont 5, B-1000 Bruxelles, Belgium.

Abstract

Thanks to excellent mechanical and biochemical properties, the nickel-titanium shape memory alloy ("Nitinol") constitutes an increasingly praised platform material in dental, cardiovascular and orthopedic biomedical devices. In order to strengthen their protective abilities towards corrosion, to reinforce their biocompatibility and to confer them specific osseointegrative capacities, Nitinol plates are covered with a thin tantalum layer by electrodeposition in the 1-butyl-1-methylpyrrolidinium bis(trifluoromethylsulfonyl)imide ionic liquid. XPS and SEM/EDX analyses highlight the chemical and morphological characteristics of the deposits: notably, these present an intrinsic dimpled nanometric structuration which is particularly remarkable considering the "soft" experimental conditions and very interesting for fundamental and applied bioactive perspectives. The present study investigates the specific and synergic effects of the Ni occurrence on the surface of the Nitinol substrates, the presence of fluorine species in the working bath, and the electrodeposition duration on the resulting formation process, morphology and chemical composition of the tantalum coating. Finally, samples are submitted to electrochemical characterizations and *in vitro* hydroxyapatite growth tests for a primary assessment of their corrosion resistance and osseoinductive features.

Keywords

Nitinol; Tantalum; Electrodeposition; 1-butyl-1-methylpyrrolidinium bis(trifluoromethylsulfonyl)imide ionic liquid; Nanostructuration.

Corresponding author

* Prof. Zineb Mekhalif, Laboratory of Chemistry and Electrochemistry of Surfaces, Facultés Universitaires Notre-Dame de la Paix (FUNDP), Rue de Bruxelles 61, B-5000 Namur, Belgium. Tel.: +32 (0)81 72 52 30. Fax: +32 (0)81 72 46 00. E-mail: zineb.mekhalif@fundp.ac.be

1. Introduction

Among the numerous kinds of shape memory alloys developed during the last 80 years for their intrinsic mechanical properties (one- and two-way shape memory phenomena, superthermoelasticity, rubber-like effect, high-damping capacity) and the number of potential application fields, the particular case of the nickel-titanium alloy constitutes one of the most promising material [1,2]. Discovered in the early 1960's by Buehler *et al.* and further known as "Nitinol" – standing for **ni**ckel-**ti**tanium (composition) and the **N**aval **O**rdnance **L**aboratory of White Oak, Maryland (place of discovery) [3], this metallic alloy can nowadays be routinely prepared under various forms (wire, bar, tubing, sheet, ribbon, strip). Depending on initial stoichiometry of Ni and Ti, presence of impurities (oxygen, carbon, nitrogen) and thermal/mechanical processing conditions and treatments during casting and shape setting processes, it can present variable and highly specific mechanical, chemical and morphological characteristics [4]. Thanks to the wide variety of its fundamental features and forces, Nitinol has quickly found an echo in numbers of advanced industrial domains – aeronautics, robotics, sensors and actuators, … – as well for many usual devices: cell-phone technology, watchmaking, sportive equipment, and even more common objects such as eyeglass frames or underwire bras [1]. But its main interest lies in the development of biomaterials for medical instruments (surgical scissors, graspers and pliers, probes) and implants in dentistry (wires, braces, screws), orthopedics (prostheses, pins, rods, plates) and cardiology (stents, heart valves) [1,2,5-8].

In this context, the main challenge concerns the biocompatibility of the nickel-titanium alloy: if titanium is widely recognized as highly biocompatible and resistant to corrosion (especially under its oxidized form TiO_2), nickel as element (usually present for ~55% in Nitinol) can easily corrode in Ni^+ and Ni^{2+} cations which have a potentially high level of toxicity, present an allergen character and are often considered as possibly carcinogen [1,5,7,8]. The biomechanical performance of bare Nitinol, mainly dependent of the host reaction induced by the material and its degradation in the body environment, is thus subject to many investigations and assessments which turn out to be very controversial: while some authors praise its good biocompatibility and its protective nature against corrosion phenomena, others are more careful and point out problems of poor bioactivity (for instance weak osseointegrative properties of several orthopedic devices), nickel leakage in human body, and implant instability – not to say long-term loosening [1,2,5,7-11]. In any case, Nitinol surface stability is the central point of those issues, and its direct control is really crucial for its further exploitation as biomaterial. Different methodologies have been pursued with this aim: some direct modifications of the oxide surface layer through mechanical, chemical and electrochemical processes (etching, sandblasting, polishing, electropolishing, anodization), heat treatments (in boiling water, air, inert gases), and surface implantations (with Ar^+, N^+, oxygen, carbon, …) have proved to act positively on the corrosion resistance, the hindering of nickel release, and the promotion of interactions with body cells and proteins [12-24].

Another convenient approach consists in the covering of Nitinol surface with organic and inorganic coatings (organosilanes and organosphophonic acids SAMs, calcium phosphate and hydroxyapatite layers, polymers and polyelectrolytes films): this strategy implies thus the creation of a barrier interface protecting the material against the potentially aggressive external conditions and preventing its damaging in the form of a nickel release from the implant to the body environment [17,24-33].

In the particular framework of orthopedic metallic biomaterials, the design of corrosion protective and osseointegrative substrates must be achieved in a synergic way. For this purpose, surface modification of Nitinol by a thin tantalum layer constitutes one of the most promising and successful methodology lately developed. Tantalum (Ta) is known for many years as a very effective material for applied biomedical perspectives owing to its total inertia towards human body, its high chemical stability and corrosion resistance, its excellent global biocompatibility and bioactivity, and also its good radiopacity [34-37]. Its use has been reported in numerous dental applications, fractures, nerves and soft tissues repairing devices, and electrodes for pacemakers [34]. However, exploitation of Ta as bulk material is restricted due to its high density and cost. The preparation of (ultra) thin Ta coatings on platform materials is thus generally preferred, for which different methods can be considered: radio frequency sputtering, chemical vapor deposition, electrostatic spray deposition, ion implantation, sol-gel coating, and electrodeposition [38-45]. This last technique has been selected here as it permits a high level of control on the composition, thickness and morphology of the deposited layer.

Originally, electrodeposition of refractory metals like Ta had to be performed in high temperature molten salts, but their utilization has been progressively limited because of strong economic and technical considerations. In presence of oxide ions, a loss in the current efficiency of the electrolysis process was noticed because of the formation of oxyfluorides which are then reduced in unstable Ta subhalides, thus the working baths had to be completely free of oxygen contaminations to lead to current efficiencies close to unity. Moreover, corrosion problems on the substrates are known to occur quicker at very high temperatures – between 650 and 850°C for Ta electrodeposition [46-48]. Recently, the use of ionic liquids media has been specifically pointed out for their advantages in terms of electrical conductivity, thermal stability, low vapor pressures and especially large electrochemical windows. In the framework of Ta electrodeposition, they also specifically allow a practical elaboration in more moderate conditions [48,49]. Several groups, including ours, have studied and commented the electrodeposition of tantalum from halide salts ($TaCl_5$ and mainly TaF_5) on platinum, gold, titanium, and Nitinol substrates, in various ionic liquids (generally imidazolium- and pyrrolidinium-based compounds) and at working temperatures between 25 and 200°C [44,45,48,50-55]. Concerning the practical conditions of electrodeposition, different electrochemical conditions have been tested. In previous papers, corresponding analyses performed with titanium substrates have shown that the Ta

layers prepared by cyclic voltammetry and potentiostatic experiments were showing very poor adherence features. However, the use of a galvanostatic deposition method (at constant current) led to very thin, homogeneous and adherent Ta films. Effects of both current density and deposition time were studied and pointed out as very important in finding a compromise between a good homogeneity of the tantalum coating and a reasonable experimental duration. Optimal values of -100 µA/cm² and 1 h at ambient temperature were found to generate the best quality Ta layers in terms of adherence, homogeneity and barrier effect [45,52].

The present paper reports the preparation on Nitinol plates of tantalum electrodeposits at ambient temperature, using an ionic liquid as solvent. Experimental conditions of electrodeposition are taken back from our previous works on pure titanium substrates [45,52]. Their particular impact, and specifically the influence of the electrodeposition time on the coatings chemical composition and morphology, is analyzed and discussed considering the particular case of the Nitinol base platform with its high nickel ratio. An evaluation of the degree of passivation and protection against corrosion brought by the Ta layer on Nitinol is also assessed through electrochemical characterizations. Finally, *in vitro* growth of hydroxyapatite crystals (inorganic part of the bone matrix) is performed on the Ta-covered substrates as a primary evaluation of the result of the surface modification on the osseoinductive properties of the material. Techniques used for the different analyses are X-ray photoelectron spectroscopy (XPS), scanning electron microscopy (SEM), energy dispersive X-rays analysis (EDX), peeling tests, free potential and polarization curves.

2. Experimental

2.1. Products and reagents

Following solvents and chemicals are used as received for the pretreatment of the Nitinol samples and the electrodeposition process of tantalum: absolute ethanol (VWR Prolabo), acetone (Chem-Lab, 99+%), ultra-pure water (18 MΩ cm), tantalum fluoride (Aldrich, 98%), and lithium fluoride (Sigma-Aldrich, ≥99%). Prior to its utilization, the ionic liquid 1-butyl-1-methylpyrrolidinium bis(trifluoromethylsulfonyl)imide (IoLiTec, 99%) is dried overnight at 100°C under 25 mbar in order to eliminate residual traces of water. The simulating body fluid (SBF) employed for the tests of *in vitro* growth of hydroxyapatite ($Ca_{10}(PO_4)_6(OH)_2$) is prepared with sodium chloride (Acros, 99.5%), potassium chloride (Aldrich, ≥99.0%), magnesium hexahydrate chloride (Acros, 99%), calcium dihydrate chloride (Merck, 99.5%), sodium hydrogenocarbonate (Acros, 99+%), potassium hydrogenophosphate (Acros, 99+%), and sodium sulfate (Jansen Chimica, 99%) [56].

2.2. Nitinol substrates preparation

Nitinol substrates considered in this study consist in intermetallic compounds and are purchased from AMF under the form of rectangular-shaped plates (20 x 10 x 0.3 mm). They are constituted of Ni (56%) and Ti (balance). The coupons are first mechanically polished on a Buehler-Phoenix 4000 instrument using silicon carbide papers (P800, then P1200) and diamond pastes (9, 3, then 1 µm) from Struers. They are then cleaned in absolute ethanol under ultrasounds for 15 min, submitted to UV-ozone for 30 min (Jelight 42-220), and finally ultrasonically retreated in absolute ethanol for 15 other min. After being blown dried under nitrogen, the substrates are stored for further use or analysis.

2.3. Tantalum electrodepositon on Nitinol surfaces

The covering of the pre-treated Nitinol plates by a Ta electrodeposit is performed in an argon-filled glove box (residual quantities of water and oxygen below 30 ppm) with an EG&G Princeton Applied Research, Potentiostat/Galvanostat Model 263A. The electrolytic solution is composed of TaF_5 0.10 M and LiF 0.25 M in the ionic liquid 1-butyl-1-methylpyrrolidinium bis(trifluoromethylsulfonyl)imide ([BMP]Tf_2N). The process is accomplished at ambient temperature (25°C) in galvanostatic conditions: a constant current of -100 µA/cm² is applied during a predefined time to the Nitinol working electrode versus a platinum foil acting as both reference and auxiliary electrodes. The modified samples are then post-treated by a copious rinsing with acetone, immersed for 15 min in boiling water, then for 15 min in absolute ethanol under ultrasounds, blown dried under nitrogen and finally submitted to UV-ozone for 15 min. For the sake of comparison, titanium (Advent, 99.98%) and nickel (Goodfellow, 99.99%) plates are also subjected to a Ta electroplating on their surfaces: pre-treatment, electrodeposition and post-treatment conditions and parameters are the same as the ones used for Nitinol substrates.

2.4. *In vitro* nucleation of hydroxyapatite

Ta-covered Nitinol substrates are immersed for 7 days at 37°C (body temperature) in 10 mL of a SBF solution of NaCl, KCl, $MgCl_2.6H_2O$, $CaCl_2.2H_2O$, $NaHCO_3$, $K_2HPO_4.3H_2O$ and Na_2SO_4 in ultra-pure water, with the following ionic concentrations (in mM): Na^+ 142.0, K^+ 5.0, Mg^{2+} 1.5, Ca^{2+} 2.5, Cl^- 148.0, HCO_3^- 4.2, HPO_4^{2-} 1.0, and SO_4^{2-} 0.5. They are then buffered at physiological pH (~7.3) with hydrochloric acid (Chem-Lab NV, 37%) and tris(hydroxymethyl)aminomethane (Acros, 98%).

2.5. XPS characterization

Surface chemical composition of the different substrates is assessed by X-ray photoelectron spectroscopy (XPS) with a Surface Science SSX-100 spectrometer. The photoelectrons are excited using a monochromatized Al Kα radiation, collected at 35° from the surface normal and detected with a hemispherical analyzer, which is operated with a pass energy of 20 eV. The spot size of the XPS source on the sample is about 600 µm, and the pressure in the analysis chamber is maintained below 1 x 10^{-9} Torr (ultra-high vacuum conditions). Binding energies of the collected peaks are made with reference to the binding energy of the C1s line at 285.0 eV, characteristic of aliphatic carbons. Their respective positions are found essentially constant from one analysis to another ($\pm$0.3 eV). Spectra are fitted using a 70-30 mix of Gaussian and Lorentzian profiles. The relative peak areas are finally measured to quantitatively characterize the different samples through elemental ratios. Sensitivity factors used for the different atoms are: C1s 1.00, O1s 2.49, F1s 3.33, Na1s 0.22, Mg2s 0.64, P2p 1.29, Cl2p 2.40, Ca2p 4.88, Ti2p 7.11, and Ta4f 9.88.

2.6. SEM imaging, EDX mapping and peeling tests procedures

A scanning electron microscope (SEM) JEOL 7500F equipped with an energy dispersive X-rays (EDX) analyzer is exploited for the visualization and the evaluation of the morphological, structural and chemical features of the different surfaces. Peeling tests to assess the adhesion aptitudes of the tantalum deposits on the Nitinol plates are performed according to the ASTM D3359 procedure: samples are scratched with a metallic comb with spacing streak of 1 mm (Elcometer 1542), then a scotch tape is stuck on the peeled surface and removed. SEM pictures of the scratched parts of the coating permit to qualitatively appraise the adhesive nature of the layer.

2.7. Electrochemical analyses (free potential and polarization curves)

Bare and modified Nitinol substrates are used as working electrodes in an electrolytic spot-cell (spot Ø: 5.2 mm), the reference and counter electrodes consisting respectively in a saturated calomel electrode (SCE, +0.246 V vs. SHE) and a platinum foil. Experiments are realized at room temperature on a EG&G Princeton Applied Research Potentiostat/Galvanostat Model VersaStat II with an electrolytic aqueous solution of 0.9%

sodium chloride (in and out gassed with nitrogen for 15 min prior to analysis). The free potential E_{free} is recorded during 30 min, then a polarization curve is measured through the scanning of the working electrode potential from -1.0 to +1.0 V/SCE at a 1 mV/s scan rate. Corrosion potential E_{cor} and corrosion current density j_{cor} are obtained by the Tafel extrapolation technique: their values correspond to the intersection of the Tafel cathodic and anodic slopes fitting the corresponding branches on the polarization curves.

3. Results and discussion

3.1. Observation: the *per se* generation of a nanostructured dimpled Ta electrodeposit on Nitinol

The development of an optimized electroplating process for the electrodeposition of tantalum (Ta) on various substrates has been the subject of a significant number of studies in the literature [44,45,48,50-55]. In the present contribution, we have directly considered a practical work at room temperature, as higher ranges (~200°C) are known to be unsuitable for thermally-sensitive substrates like Nitinol shape memory alloy and to encourage the faster degradation of the electrolytic solution (especially tantalum fluoride) [52]. As the deposition of Ta is also directly influenced by the selected ionic liquid, especially near ambient temperature, we have chosen to work in 1-butyl-1-methylpyrrolidinium bis(trifluoromethylsulfonyl)imide ([BMP]Tf_2N), which has been acknowledged for its efficiency at this purpose [53,54]. Molar concentrations of the TaF_5 precursor and the LiF additive specie (which specifically facilitates the electrodeposition of thin crystalline tantalum layers [50]) have been respectively fixed at 0.10 and 0.25 M [52].

The Ta element is well known in the literature to present highly complicated electrodeposition behaviors regarding the selected experimental conditions (substrate, ionic liquid, temperature, …) [44,45,50,51,53,54]. In order to investigate the electrochemical reactivity of the electrodeposition bath, a cyclic voltammogram is recorded in this electrodeposition solution (i.e. 0.25 M LiF / [BMP]Tf_2N), with and without the presence of 0.10 M TaF_5 (Fig. 1). This experiment is carried out at room temperature and under controlled atmosphere (glove box). The electrode potential is scanned at a rate of 100 mV/s between -3 and +2 V/Pt, starting from open circuit potential (0 V/Pt) with a negative initial scan polarity. In presence of the tantalum salt, the cathodic process includes two reduction waves. The first one (R1) is observed until -1.5 V/Pt and can be correlated to the first reduction of Ta(+V) to Ta(+III), as the TaF_3 compound is known for its stability [44,50,51]. The second wave (R2), starting from -1.5 V/Pt, is attributed to the electrodeposition of metallic tantalum Ta(0). On the reverse scan, the progressive dissolution of the Ta layer into different TaF_x compounds ($x \leq 5$) is highlighted towards three main oxidative processes. The first slight current peak at -1.2 V/Pt (O1) corresponds to the dissolution of Ta(0) into assumed non-stoichiometric TaF_x subhalides, with $0 < x \leq 2$ [51,54]. Then the second broad peak centered at +0.2 V/Pt (O2) corresponds to the transformation into the stable Ta(+III) form as TaF_3. Finally, the last oxidation wave starting from +1.2 V/Pt (O3) corresponds to the complete reconversion into Ta(+V) as TaF_5. Similar global trends were previously noticed by cyclic voltammetry for the electrodeposition process of Ta onto Pt, Au and Ti [44,45,48,50-54].

Correspondingly with our previous works on titanium substrates [45,52], both cyclic voltammetry and constant potential methods tested with Nitinol as substrate result in very poorly adherent Ta deposits (not shown here): indeed, the simple rinsing of the surface with

acetone immediately after the electrodeposition provokes an almost complete removing of the thin tantalum film. Nevertheless, constant current experiments emerge as more noticeable and conclusive. Fig. 2a-c presents SEM images of a Ta film electrodeposited on a Nitinol plate at -100 µA/cm² during 1 h (optimized conditions taken back from the case of a Ti substrate). Very interestingly, the electrodeposit consists in an intrinsically-structured layer presenting regular and well-defined circular nanometric cavities (Ø ~ 100-200 nm). This structure is present on the whole Ta surface covering the Nitinol sample and is observed with high degree of reproducibility. The coatings are moreover well adherent to the substrate surface, as confirmed by the SEM pictures recorded after peeling tests (Fig. 3).

The *per se* generation of this kind of hollowed structuration is very remarkable, especially considering those current parameters: if the preparation and development of high-definition micro- and nanostructures on surfaces have been essentially studied and performed through anodization processes, generally with strong technical constraints (high voltages, aggressive environments, …), it is the first time – to the best of our knowledge – that cathodic current "soft" conditions lead to the formation of ordered porous structures, and more particularly with electrodeposits. Beyond these fundamental considerations, the specific and controlled structuration of the material is strongly sought here for its beneficial nature in terms of further bioactivity: in addition to confer reinforced integrative aptitudes to the biomaterial via a stronger "Velcro effect" (especially for the osseous regrowth with orthopedic repairing devices), those cavities can also act as preferred sites for the nucleation of hydroxyapatite crystals and the attachment process of body cells. The fundamental intrinsic ability of those Nitinol substrates in generating natively-structured deposits could thus be hugely interesting and worthy for applied perspectives, as it should in this case allow the bypass of energy-, cost- and time-demanding methodologies of surface nanostructuration like anodization or template-assisted formation of inverse porous structures [23,52].

To our opinion, one of the main reasons at the root of this intrinsic nanostructuration stands in the chemical nature of the underlying substrate: indeed, with Ti plates as platforms (Fig. 4a-b) [45,52], complete, homogeneous and compact Ta electrodeposits are obtained, presenting no evidence of any kind of (intrinsic) nanostructure. As a comparison, tests of tantalum electrodeposition on Ni substrates (Fig. 4c-d) lead to incomplete layers, with areas covered by thin granuleous Ta deposits (zones in light grey on Fig. 4d) and others uncovered, as testified by the observation of residual polishing scratches (zones in dark grey on Fig. 4d). In the case of Nitinol, the observation of nanometric hollows on the Ta electrodeposits covering the samples seems thus to be an original and specific effect of the "cohabitation" of Ni and Ti elements, resulting in an intrinsic structuration phenomenon. However, this statement cannot be considered as a generality for all kinds of nickel-titanium shape memory alloys: in a previous study, the precise case of the tantalum electrodeposition on Nitinol has already been investigated, and the formation of dense and adherent layers containing fine crystallites was reported [44]. The aspect and morphology of those coatings

have no clear correspondence with the ones presented here, but this can probably be explained by the exploitation of different experimental conditions between the two situations: electrochemical processes (potentiostatic deposition at -2.0 V/Pt vs. galvanostatic deposition at -100 µA/cm²), working temperatures (200 vs. 25°C), TaF_5 concentrations (0.25 vs. 0.10 M) and essentially Nitinol substrate shapes and relative elemental compositions (wire vs. plate, 50-50 vs. 56-44 for Ni/Ti ratios). It seems thus obvious that a good grasp of fundamental and practical parameters, and mainly those concerning the Nitinol substrate mechanical and chemical characteristics, combined with a suitable definition and optimization of the experimental conditions for the electrodeposition process can have a direct and critical impact on the structural and morphological properties of the resulting Ta film.

The chemical nature of the tantalum-Nitinol interface must be carefully examined at this stage. Fig. 5 shows the XPS survey spectrum (a) and the Ta4f (b), F1s (c), Ti2p (d), and Ni2p (e) core levels of a Nitinol substrate covered with tantalum after electrodeposition at -100 µA/cm² during 1 h. The coating on the surface is clearly present and is obviously constituted of tantalum pentoxide, as testified by the binding energy E_b of 26.6 eV measured for the Ta4f signal: due to the high affinity of metallic tantalum for oxygen, the Ta layer is directly oxidized in Ta_2O_5 as soon as it is exposed to the ambient atmosphere. Moreover, no residual traces of TaF_5 are anymore detected (above 27 eV). Concerning fluorine compounds, XPS analyses also reveal a very slight contamination despite the post-treatment protocol, with the occurrence of a small F1s peak at 688.6 eV. The specific question of the origin and consequences of the presence of F will be discussed in details in the next section. Ti2p and Ni2p peaks, characteristic of the underlying Nitinol platform, are also observed: they indicate that the Ta layer thickness should be lower than 10 nm, which is the value of the depth detection limit of the XPS spectrometer. Despite the fact that a cathodic – thus reducing – current has been applied during the electrodeposit process, both titanium and nickel elements are identified in their oxidized form: TiO_2 for Ti2p (E_b = 459.0 eV) and Ni_2O_3/$Ni(OH)_2$ for Ni2p (E_b = 856.5 eV), respectively. This should mean that a thin layer of nickel and titanium oxides is still present at the extreme surface of the Nitinol substrate, just at the interface with the dimpled tantalum deposit. This “non-reduction” phenomenon is not surprising in the case of titanium dioxide, whose stability and passive nature are strong enough to resist to such a weak reductive current. However, oxidized nickel present at the surface of Nitinol should have been immediately reduced by the application of this cathodic current simultaneously to the electrodeposition of tantalum, which is obviously not the case. An explanation to this stands probably in the fact that a portion of the underlying nickel remains in contact with the external atmosphere after the Ta covering and is directly reoxidized when exposed to ambient air. Considering that the coating covers the Nitinol sample all over its surface, the only small access pathways that could exist between the Nitinol substrate – more precisely the Ni element – and the external environment lie in the nanometric hollows in the Ta layer. Indeed, tantalum is well detected on their inner surface

on EDX mappings (Fig. 6) but the coverage is probably not complete, which could thus lead to a direct link between the extreme surface of the underlying Nitinol and the ambient atmosphere. Further experimental investigations are planned in this connection to precisely describe and discuss the internal structure of the porous Ta film.

3.2. Investigation: the qualitative and quantitative evaluation of the surface chemical composition in the perspective of the formation process of the dimpled Ta layer

Primary observations previously noticed clearly establish a link between the elemental constitution of the tantalum-Nitinol interface and the corresponding topographic and morphological features of the surface coating. Thus it appears important to study these aspects in the perspective of the formation process of the tantalum electrodeposit on Nitinol. Two key parameters are considered hereafter: the composition of the working solution in terms of fluoride ions and the electrodeposition time. SEM and XPS analyses on modified Nitinol samples are achieved for this purpose. The specific impact of the presence of fluorine compounds in the reaction bath on Nitinol surfaces is studied through “blank” experiments in solutions containing no tantalum precursor. Concerning the deposition time, the Nitinol substrates are submitted to different Ta electroplating durations, going from 10 min to 2 h.

The first point of discussion resides in the slight residual presence of fluorine in the chemical constitution of the extreme surface. To our opinion, this is directly related to the use of Nitinol plates as substrates (indeed, no F signal was detected in the case of Ti samples [45,52]). Furthermore, it may have an important effect on the formation, structuration, composition and final aspect of the tantalum electrodeposits. In the biomedical field, and especially in fundamental and applied dentistry fields, fluorine compounds are well known for their active therapeutic properties, for which they are commonly incorporated in numerous drugs and hygienic products (such as toothpastes) in small quantities. However, the substantial toxicity of F as element – and particularly F^- ions – when moderate-to-large concentrations are involved is particularly disquieting: its use must thus be considered and regulated with high attention and precaution. In the particular framework of titanium and its alloys – especially Nitinol – used as bulk biomaterials, a direct contact with specific fluoride ions-containing solutions has proved to be potentially generative of a breakdown of the protective passivation layer accompanied by the formation and dissolution of halide complexes, resulting in the localized or generalized corrosion of the material [57-62]. With the present experimental situation, implying different sources of fluoride ions in the working electrodeposition solution (TaF_5 and LiF), the possibility of a direct interaction between F^- entities and the sensitive Nitinol substrates is highly conceivable. In order to investigate those potential problems, experiments have been realized in blank solutions containing no tantalum source (TaF_5). Nitinol samples have thus been immersed in a 0.25 M LiF solution in

[BMP]Tf_2N for 1 h at room temperature, with and without the application of the -100 µA/cm² current density exploited in the tantalum electrodeposition protocol. Table 1 lists the Ni2p/Ti2p ratios of the considered samples after XPS investigations: a net decrease of the value is noticed from bare (~1.0) to modified Nitinol plates (~0.4), which corresponds obviously to an erosion phenomenon of Ni entities by the F^- ions directly coming from the LiF additive specie. Observation of SEM pictures of the fluorine-altered substrates and comparison with bare Nitinol samples tend to confirm this erosive behavior: as well with (Fig. 7a-b) as without (Fig. 7c-d) application of a cathodic current density, very discreet and fine nanometric hollows are founded all over the samples surface, which is subtly observed on high magnification images of modified substrates (Fig. 7b and 7d) and not on pristine Nitinol plates (Fig. 7e). Those observations lead us to consider the abrasive action of the F^- ions on the bare Nitinol surfaces as a precursor step of the intrinsic nanostructuration process, with small nanometric gaps induced by fluorides acting then as template sites for the ulterior deposition of tantalum and the final generation of a structured porous coating.

Now that the role and impact of the F^- ions are clarified, we need to explore their incidence on the progressive formation of the tantalum films. A specific investigation of the samples chemical composition and morphology is thus considered for various electrodeposition times, going from 10 min to 2 h. As previously, the current density value applied during the experiment remains equal to -100 µA/cm². With regard to SEM images on Fig. 8, the formation process can be subdivided into different main steps. The first signs of the presence of the Ta layer are noticed after 10 min (Fig. 8a) with the observation of a thin granuleous deposit of tantalum and the very beginning of the pores digging (as seen at the bottom of Fig. 8a). Then the hollowed coating is gradually formed (from 15 to 30 min, Fig. 8b-d) with the progressive definition of the cavities quantity, size and form. In a further stage, the intrinsic nanostructuration of the film continues and fines down (from 40 to 60 min, Fig. 8e-f): the pores surface density keeps growing (from 2.0 10^9 pores/cm² after 30 min to 4.5 10^9 pores/cm² after 60 min) while their dimensions and shape become increasingly better defined. After 1 h of electrodeposition, a complete Ta dimpled layer consistently covers the entire Nitinol surface, with hollows presenting a regular circular form of an average diameter of 120 nm. On longer durations, we observe a gradual filling of the cavities by tantalum (90 min, Fig. 8g) as the surface pores density and diameter starts to decrease (down to 1.8 10^9 pores/cm² and 67 nm, respectively) with the appearance of a compact and homogeneous layer progressively covering the underlying hollowed structure, which remains observable here and there (120 min, Fig. 8h). The thickening and completion of the tantalum coating with the electrodeposition time is confirmed by the different XPS Ta4f/(Ti2p+Ni2p) elemental ratios (Table 2), starting from 2.4 after 10 min, stagnating between 2.7 and 2.9 until 1 h, and drastically increasing with longer durations (up to be innumerable for a 120 min time because of the disappearance of the Ti2p and Ni2p signals – characteristic of the Nitinol substrate – on the spectra). Besides, the evolution of the Ni2p/Ti2p ratio with the electrodeposition time is particularly instructive (Table 2). Short times (10 and 15 min)

results in a deficient Ni proportion (Ni/Ti < 1), which can be attributed to its abrasion by the fluoride ions present in solution (as demonstrated before). However, extended durations show an increasing of the Ni quantity, with ratios going from 1.7-1.9 (20-40 min) to 3.0 (60 min). Concerning the behavior of the Ni2p/Ta4f ratio (Table 2), it starts from relatively weak values at short electrodeposition times (~0.2), indicating the strong erosion of the Ni element by fluorides. Then it rises up to ~0.7 after 20 and 30 min of electrodeposition, which can be explain by a trapping phenomenon of nickel-containing species between the Nitinol platform and the tantalum electrodeposit in formation. Finally, the ratio value decreases back to ~0.3 for longer durations (40 min and more), probably due to the variation of the XPS analysis depth because of the progressive increase of the Ta quantity deposited on the surface. The elemental Ni enrichment of the extreme surface with time, and their residual detection on XPS spectra, seems thus to be a consequence of the simultaneity of the electrodeposition of tantalum and the abrasion of nickel from the Nitinol surface, resulting in a kind of incorporation of the mobile nickel (and fluorine) various compounds at the interface between the substrate and the coating. The possibility of a Ni diffusion phenomenon from Nitinol bulk to the surface, resulting from the fluorides action and/or the electrode polarization, can also be invoked as hypothesis.

As a preliminary conclusion, we can stipulate that those experimental results and the different deriving interpretations are rich of lessons. On the one hand, it seems clear that the presence of Ni at the surface of the Nitinol substrate and its erosion by fluoride ions contained in the electrodeposition bath positively influence the morphology of the Ta coating by conferring it an intrinsic porous nanostructuration in “soft” cathodic current conditions. On the other hand, the resulting Ni enrichment of the extreme surface combined with its potential accessibility from the external atmosphere via the weakly-Ta-covered pores pose direct interrogations concerning the consequences on substrate sensitivity to corrosion and biocompatibility, which truly deserve to be answered and solved through further studies.

3.3. Potentiality: the role of the Ta coating in the protection and the “biofunctionalization” of Nitinol

The final part of this work is expressly devoted to the evaluation of the Ta electrodeposit properties and functionalities: electrochemical characterizations are carried out to quantify the extent of the provided barrier effect against Nitinol corrosion in NaCl aqueous solutions, while bioactivity and primary osseoinductive properties are assessed with the accomplishment of *in vitro* hydroxyapatite (HAp) growth tests. Experimental conditions for the electrodeposition of Ta on Nitinol still consist in the application of a current density of -100 µA/cm² during 1 h at 25°C.

Free potential and polarization curves of bare (NiTi) and Ta-covered Nitinol (NiTi-Ta) samples are showed on Fig. 9. The passivative nature of the deposit is demonstrated: an average

value of -67 mV/SCE is measured for the E_{free} of NiTi-Ta, which represents a substantial increase from the -257 mV/SCE value recorded for NiTi (Fig. 9a and Table 3). Regarding polarization curves (Fig. 9b and Table 3), a noticeable decrease is remarked for the corrosion current density j_{cor} (from 15.2 to 2.34 10^{-8} A/cm² with bare NiTi): this also testifies for a good ability of the Ta layer in hindering corrosion processes. This inhibitive behavior presents a cathodic character, with a displacement of the corrosion potential value E_{cor} from -355 mV/SCE with NiTi to -529 mV/SCE with NiTi-Ta. Both anodic and cathodic branches current densities of NiTi-Ta substrates remain comparable to their NiTi homologues at extreme potentials, but decreases to some extent at potentials around E_{cor} (between -700 and +200 mV/SCE). Despite their relative thinness – a few nm – and their dimpled nature, suggesting a latent access of nickel species to the external environment, the so-prepared Ta films present slender abilities of passivation and a barrier effect against corrosion in these standard primary testing conditions. Usually, thicker Ta-based deposits are considered for corrosion protection of sensitive metallic substrates (from 100 nm to several µm) [41,44], but very thin coatings can also be aimed: for instance, Marcus *et al.* have recently shown that ultra-thin coatings of Ta_2O_5 (from 5 to 50 nm) prepared by atomic layer deposition could be considered for the protection of 316L stainless steel plates [63]. In any case, the extent of the potential beneficial trends brought by such thin Ta electrodeposits on Nitinol must be confirmed by further advanced corrosion investigations.

The estimation of the hydroxyapatite growth ability of the Ta-coated Nitinol samples after their immersion for 7 days at 37°C and pH ~ 7.3 in the SBF solution is achieved by SEM/EDX and XPS analyses. Microscopic images (Fig. 10) reveal the presence on the dimpled Ta surface of punctual HAp crystals, whose chemical nature is confirmed by EDX mappings on Fig. 11 (with the measurement of substantial signals for Ca and P elements). The crystals exhibit a kind of circular “gypsum flower” morphology with a diameter of ~ 1 µm. The corresponding XPS survey spectrum (Fig. 12) confirms the occurrence of HAp on the surface with the detection of characteristic Ca2p (E_b = 347.8 eV) and P2p (E_b = 133.5 eV) signals and the calculation of an experimental 1.74 value for the Ca2p/Ti2p ratio corresponding to the theoretical one (1.67). Other constitutive elements of the SBF solution (Na, Mg, Cl) are also residually observed. As a result, this first bioactivity assay highlights the good primary osseoinductive properties of a Ta film on Nitinol plates, and opens the way to further advanced biological and medical tests.

4. Conclusions

The present study intends to develop an efficient and fine strategy for an optimized exploitation of the nickel-titanium shape-memory alloy as orthopedic biomaterial platform. The global objective consists in the enhancement of the fundamental mechanical, physical and biochemical advantages of Nitinol through the strengthening of its barrier effect properties against corrosive media, the consolidation of its biocompatibility and the reinforcement of its osseoinductive abilities. Electrodeposition of thin tantalum coatings in ionic liquid solutions has been conducted for this purpose: tantalum as covering metal presents highly interesting characteristics in terms of corrosion resistance and bioactivity, and electrodeposition as working methodology is highly appreciated for its large control capacities on the resulting thickness, aspect and composition of the deposits. Moreover, ionic liquids as solvents allow a more practical work in moderate experimental conditions. Electrodeposition parameters are taken back from similar studies performed on titanium substrates and are applied to the particular case of Nitinol. More precisely, galvanostatic experiments are performed considering definite current and time parameters: they lead to the deposition of thin and adherent films presenting a regular and well-defined dimpled morphology. Their formation process has also been described in function of the deposition duration: different main steps have been identified in the light of morphological and chemical assessments. The intrinsic nature of this *in situ* nanostructuration of the deposited tantalum is particularly remarkable considering the cathodic “soft” current settings and very interesting for osseointegrative purposes, as confirmed by the *in vitro* hydroxyapatite growth assays. We specifically manage to point out that this *per se* behavior is fundamentally associated to the occurrence of the nickel element on the extreme surface of the substrates: fluorine compounds contained in the electrodeposition bath have been identified as reactive species towards Nitinol, causing a leakage phenomenon of Ni ions and the slight nanometric erosion of the surface. If the impact on the morphological features of the Ta coating has been highlighted as clearly beneficial, it must be considered in the light of the parallel drawback potentially caused by the Ni and F enriching in the tantalum-Nitinol interface, which raises several questions in terms of toxicity and corrosion propensity.

Among the different applied perspectives of this work, extended corrosion assays can be achieved through the analysis of the samples behavior in more restrictive environments, while the assessment of the substrates bioactivity can be completed with further tests of adhesion, proliferation and cytotoxicity of osteoblasts and osteoclasts osseous cells.

Acknowledgment

A. Maho is grateful to FNRS-FRIA for fellowship.

References

[1] D. Mantovani, JOM-J. Min. Met. Mat. S. 52 (2000) 36.

[2] F. El Feninat, G. Laroche, M. Fiset, D. Mantovani, Adv. Eng. Mater. 4 (2002) 91.

[3] W.J. Buehler, R.C. Wiley, U.S. Patent 3,174,851 (1965).

[4] M.H. Elahinia, M. Hashemi, M. Tabesh, S.B. Badhuri, Prog. Mater. Sci. 57 (2012) 911.

[5] S.A. Shabalovskaya, BioMed. Mater. Eng. 6 (1996) 267.

[6] T. Duerig, A. Pelton, D. Stöckel, Mater. Sci. Eng. A273-275 (1999) 149.

[7] M. Balazic, J. Kopac, M.J. Jackson, W. Ahmed, Int. J. Nano and Biomaterials 1 (2007) 3.

[8] M. Geetha, A.K. Singh, R. Asokamani, A.K. Gogia, Prog. Mater. Sci. 54 (2009) 397.

[9] J. Ryhanen, E. Niemi, W. Serlo, E. Niemela, P. Sandvik, H. Pernu, T. Salo, J. Biomed. Mater. Res. 35 (1997) 451.

[10] S.A. Shabalovskaya, BioMed. Mater. Eng. 12 (2002) 69.

[11] M. Es-Souni, M. Es-Souni, H. Fischer-Brandies, Anal. Bioanal. Chem. 381 (2005) 557.

[12] C. Trépanier, T.K. Leung, M. Tabrizian, L'H. Yahia, J.-G. Bienvenu, J.-F. Tanguay, D.L. Piron, L. Bilodeau, J. Biomed. Mater. Res. 48 (1999) 165.

[13] L. Tan, R.A. Dodd, W.C. Crone, Biomaterials 24 (2003) 3931.

[14] S. Shabalovskaya, G. Rondelli, J. Anderegg, J. P. Xiong, M. Wu, J. Biomed. Mater. Res. B 69 (2004) 223.

[15] N. Shevchenko, M.-T. Pham, M.F. Maitz, Appl. Surf. Sci. 235 (2004) 126.

[16] B. Clarke, W. Carroll, Y. Rochev, M. Hynes, D. Bradley, D. Plumley, J. Biomed. Mater. Res. A 79 (2006) 61.

[17] S. Shabalovskaya, J. Anderegg, J. Van Humbeeck, Acta Biomater. 4 (2008) 447.

[18] W. Chrzanowski, E.A.A. Neel, D.A. Armitage, J.C. Knowles, Acta Biomater. 4 (2008) 1969.

[19] S. Shabalovskaya, G. Rondelli, M. Rettenmayr, J. Mater. Eng. Perform. 18 (2009) 470.

[20] L.M. Perez, L. Gracia-Villa, J.A. Puertolas, M. Arruebo, S. Irusta, J. Santamaria, J. Biomed. Mater. Res. B 91 (2009) 337.

[21] W. Simka, M. Kaczmarek, A. Baron-Wiechec, G. Nawrat, Jan Marciniak, J. Zak, Electrochim. Acta 55 (2010) 2437.

[22] Z. Bai, H.H. Rotermund, J. Biomed. Mater. Res. B 99 (2011) 1.

[23] S.A. Bernard, V.K. Balla, N.M. Davies, S. Bose, A. Bandyopadhyay, Acta Biomater. 7 (2011) 1902.

[24] S. Devillers, B. Barthélémy, J. Delhalle, Z. Mekhalif, ACS Appl. Mater. Interfaces 3 (2011) 4059.

[25] X. Kong, R.G. Grabitz, W. van Oeveren, D. Klee, T.G. van Kooten, F. Freudenthal, M. Qing, G. von Bernuth, M.-C. Seghaye, Biomaterials 23 (2002) 1775.

[26] D. Budziak, E. Martendal, E. Carasek, J. Chromatogr. A 1164 (2007) 18.

[27] C. Hessing, J. Frenzel, M. Pohl, S. Shabalovskaya, Mater. Sci. Eng. A 486 (2008) 461.

[28] T.D. Sargeant, M.S. Rao, C.-Y. Koh, S.I. Stupp, Biomaterials 29 (2008) 1085.

[29] G. Zorn, R. Adadi, R. Brener, V.A. Yakovlev, I. Gotman, E.Y. Gutmanas, C.N. Sukenik, Chem. Mater. 20 (2008) 5368.

[30] F. Sun, K.N. Sask, J.L. Brash, I. Zhitomirsky, Colloid. Surface. B 67 (2008) 132.

[31] R. Quinones, E.S. Gawalt, Langmuir 24 (2008) 10858.

[32] D. Zhang, W. Zeng, Z. Zi, P.K. Chu, Mater. Sci. Eng. C 29 (2009) 1599.

[33] D. Qiu, L. Yang, Y. Yin, A. Wang, Surf. Coat. Technol. 205 (2011) 3280.

[34] J. Black, Clin. Mater. 16 (1994) 167.

[35] D.C.N. Chan, H.W. Titus, K.-H. Chung, H. Dixon, S.T. Wellinghoff, H.R. Rawls, Dent. Mater. 15 (1999) 219.

[36] T. Miyazaki, H.-M. Kim, T. Kokubo, C. Ohtsuki, H. Kato, T. Nakamura, Biomaterials 23 (2002) 827.

[37] V.K. Balla, S. Bodhak, S. Bose, A. Bandyopadhyay, Acta Biomater. 6 (2011) 3349.

[38] Y. Imai, A. Watanabe, M. Mukaida, K. Osato, T. Tsunoda, T. Kameyama, K. Fukuda, Thin Solid Films 261 (1995) 76.

[39] C. Corbella, M. Vives, A. Pinyol, I. Porqueras, C. Person, E. Bertran, Solid State Ionics 165 (2003) 15.

[40] A. Lintanf, A. Mantoux, E. Blanquet, E. Djurado, J. Phys. Chem. C 111 (2007) 5708.

[41] T. Zhao, R. Yang, C. Zhong, Y. Li, Y. Xiang, J. Mater. Sci. 46 (2011) 2529.

[42] S. Yildirim, K. Ulutas, D. Deger, E.O. Zayim, I. Turhan, Vacuum 77 (2005) 329.

[43] A. Maho, S. Linden, C. Arnould, S. Detriche, J. Delhalle, Z. Mekhalif, J. Colloid Interface Sci. 371 (2012) 150.

[44] S. Zein El Abedin, U. Welz-Biermann, F. Endres, Electrochem. Commun. 7 (2005) 941.

[45] C. Arnould, J. Delhalle, Z. Mekhalif, Electrochim. Acta 53 (2008) 5632.

[46] S. Senderoff, G.W. Mellors, W.J. Reinhart, J. Electrochem. Soc. 112 (1965) 840.

[47] P. Chamelot, P. Palau, L. Massot, A. Savall, P. Taxil, Electrochim. Acta 47 (2002) 3423.

[48] T. Schubert, S. Zein El Abdein, A.P. Abbott, K.J. McKenzie, K.S. Ryder, F. Endres, in: F. Endres, A.P. Abbott, D.R. MacFarlane (Eds.), Electrodeposition from Ionic Liquids, Wiley-VCH, Weinheim, Germany, 2008, pp. 83-123.

[49] A.P. Abbott, I. Dalrymple, F. Endres, D.R. MacFarlane, in: F. Endres, A.P. Abbott, D.R. MacFarlane (Eds.), Electrodeposition from Ionic Liquids, Wiley-VCH, Weinheim, Germany, 2008, pp. 1-13.

[50] S. Zein El Abedin, H.K. Farag, E.M. Moustafa, U. Welz-Biermann, F. Endres, Phys. Chem. Chem. Phys. 7 (2005) 2333.

[51] N. Borisenko, A. Ispas, E. Zschippang, Q. Liu, S. Zein El Abedin, A. Bund, F. Endres, Electrochim. Acta 54 (2009) 1519.

[52] C. Arnould, J. Delhalle, Z. Mekhalif, J. Electrochem. Soc. 156 (2009) K186.

[53] F. Endres, O. Höfft, N. Borisenko, L.H. Gasparotto, A. Prowald, R. Al-Salman, T. Carstens, R. Atkin, A. Bund, S. Zein El Abedin, Phys. Chem. Chem. Phys. 12 (2010) 1724.

[54] A. Ispas, B. Adolphi, A. Bund, F. Endres, Phys. Chem. Chem. Phys. 12 (2010) 1793.

[55] O.B. Babushkina, S. Ekres, Electrochim. Acta 56 (2010) 867.

[56] D. Krupa, J. Baszkiewicz, J.W. Sobczak, A. Bilinski, A. Barcz, J. Mater. Process. Technol. 143-144 (2003) 158.

[57] F. Toumelin-Chemla, F. Rouellei, G. Burdairon, J. Dent. 24 (1996) 109.

[58] L. Reclaru, J.-M. Meyer, Biomaterials 19 (1998) 85.

[59] N. Schiff, B. Grosgogeat, M. Lissac, F. Dalard, Biomaterials 23 (2002) 1995.

[60] M. Cioffi, D. Gilliland, G. Ceccone, R. Chiesa, A. Cigada, Acta Biomater. 1 (2005) 717.

[61] X. Li, J. Wang, E.-h. Han, W. Ke, Acta Biomater. 3 (2007) 807.

[62] B. Bozzini, A. Gianoncelli, B. Kaulich, M. Kiskinova, C. Melea, M. Prascioluc, Phys. Chem. Chem. Phys. 13 (2011) 7968.

[63] B. Diaz, J. Swiatowska, V. Maurice, A. Seyeux, B. Normand, E. Harkonen, M. Ritala, P. Marcus, Electrochim. Acta 56 (2011) 10516.

Figures

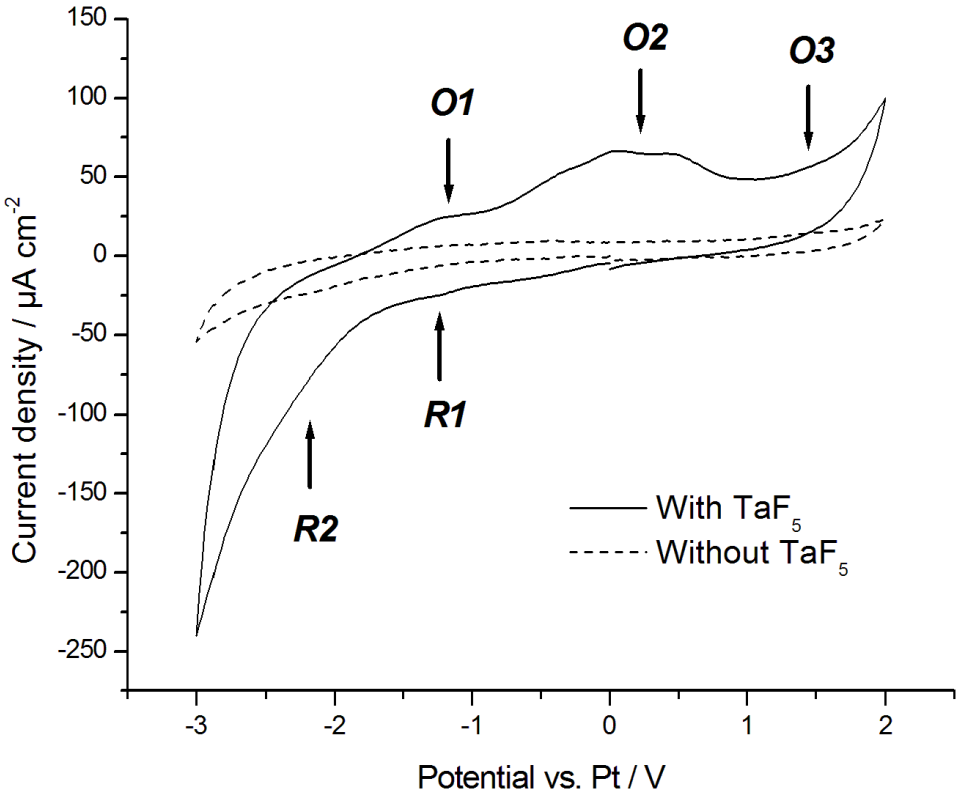

Fig. 1. Cyclic voltammogram of a Nitinol substrate in a 0.25 M LiF solution in [BMP]Tf_2N, with (plain line) and without (dash line) the presence of 0.10 M TaF_5. The curves are recorded at a scan rate of 100 mV/s and at room temperature (25°C).

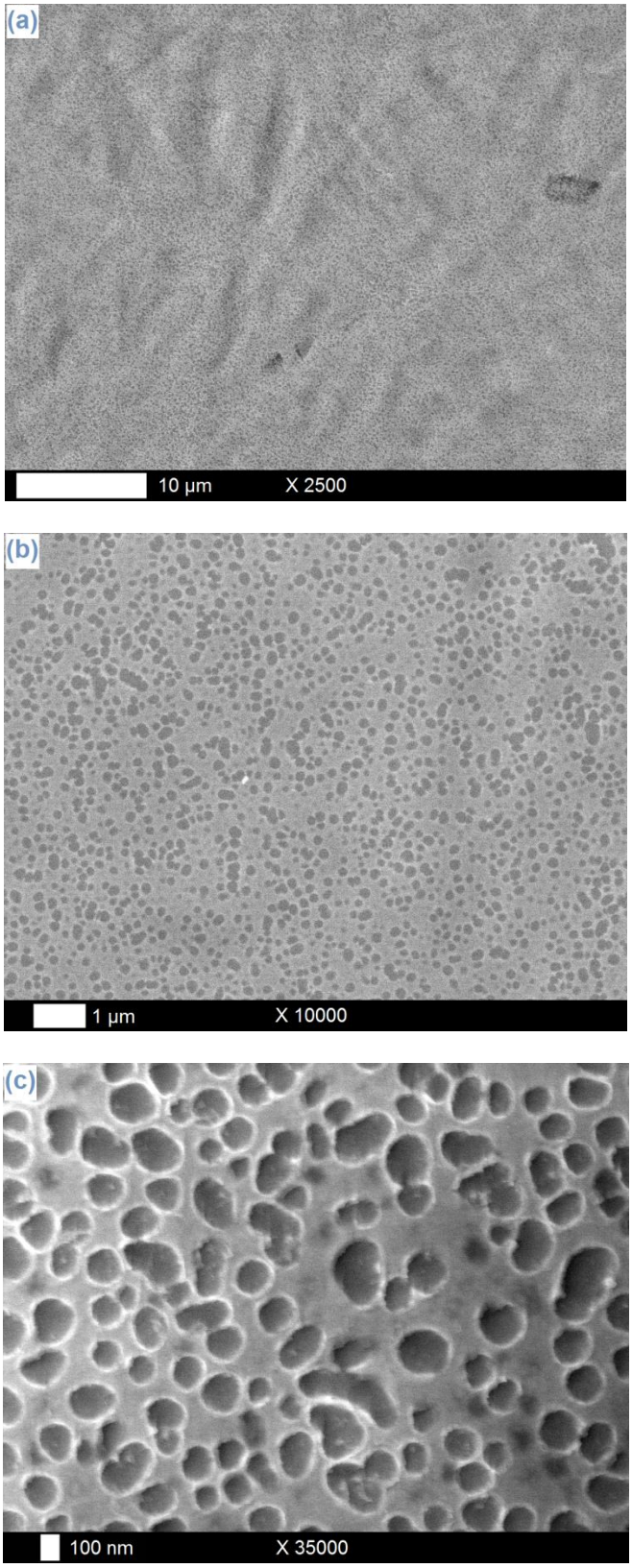

Fig. 2a-c. SEM pictures of Ta layers galvanostatically electrodeposited on Nitinol plates at -100 µA/cm², 25°C and during 1 h.

Fig. 3. SEM picture of Ta layers electrodeposited on Nitinol plates, after peeling test.

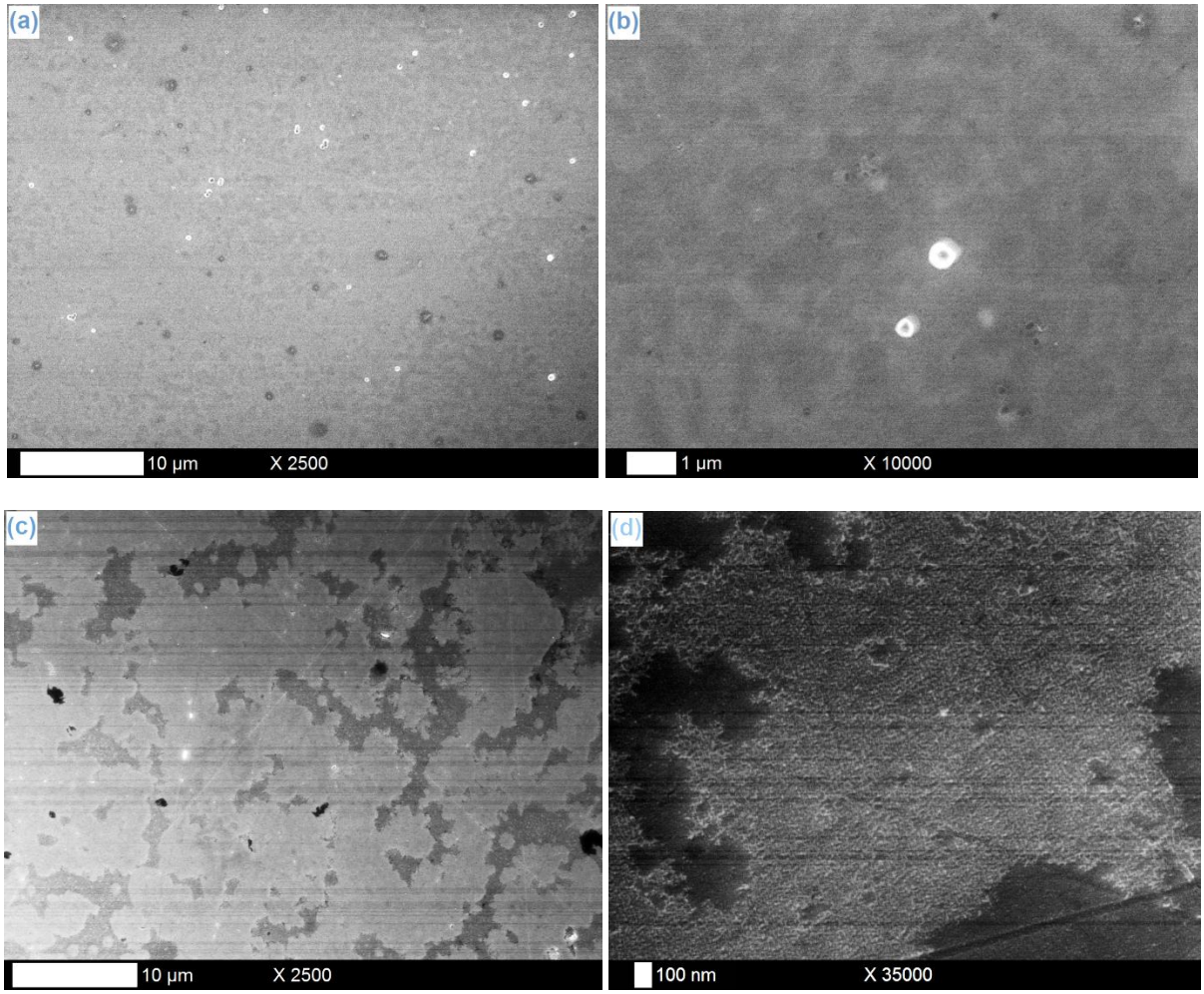

Fig. 4. SEM pictures of Ta layers galvanostatically electrodeposited on titanium (a-b) and nickel (c-d) plates at -100 µA/cm², 25°C and during 1 h.

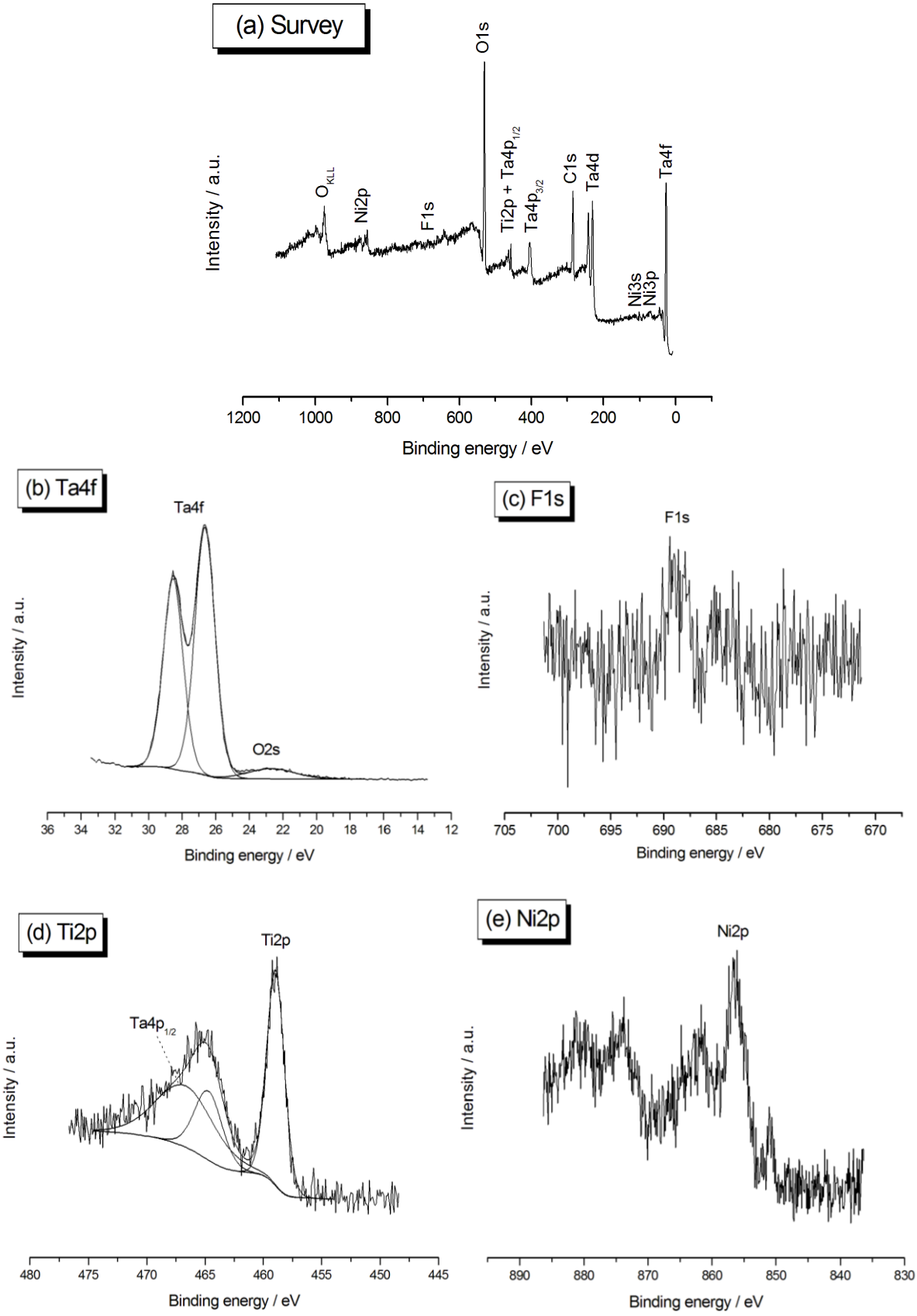

Fig. 5. XPS survey spectrum (a) and Ta4f (b), F1s (c), Ti2p (d), and Ni2p (e) core levels of a Nitinol substrate covered by a Ta electrodeposit.

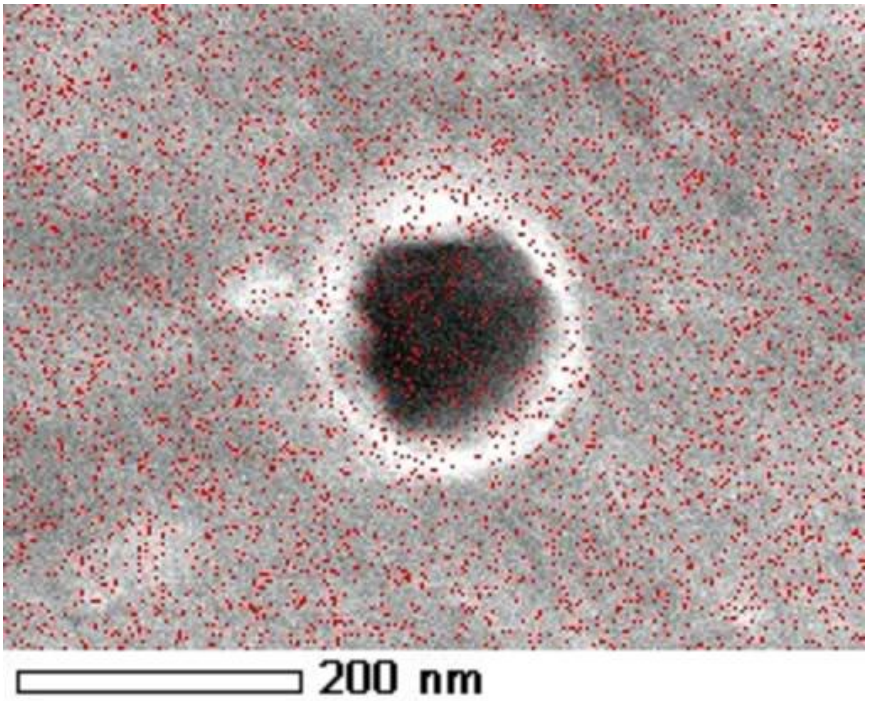

Fig. 6. EDX mapping (red spots highlight Ta presence – Ta M signal) of one pore in the Ta layer covering a Nitinol substrate.

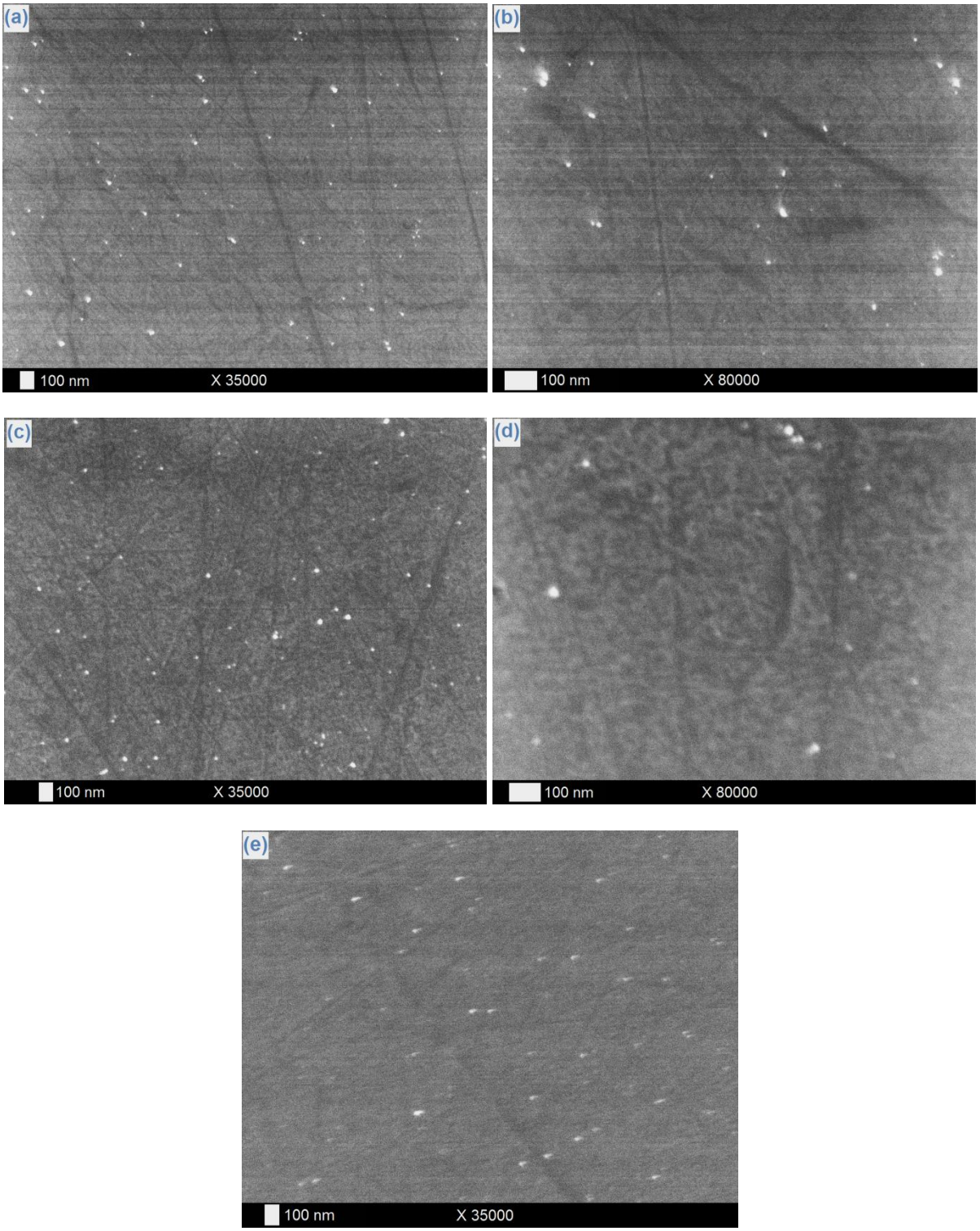

Fig. 7. SEM pictures of Nitinol surfaces after contact with a 0.25 M LiF / [BMP]Tf_2N solution during 1 h at 25°C (a-b) with an applied current density of -100µA/cm² and (c-d) in open circuit conditions (without current). Bare Nitinol surfaces are also presented for the sake of comparison (e).

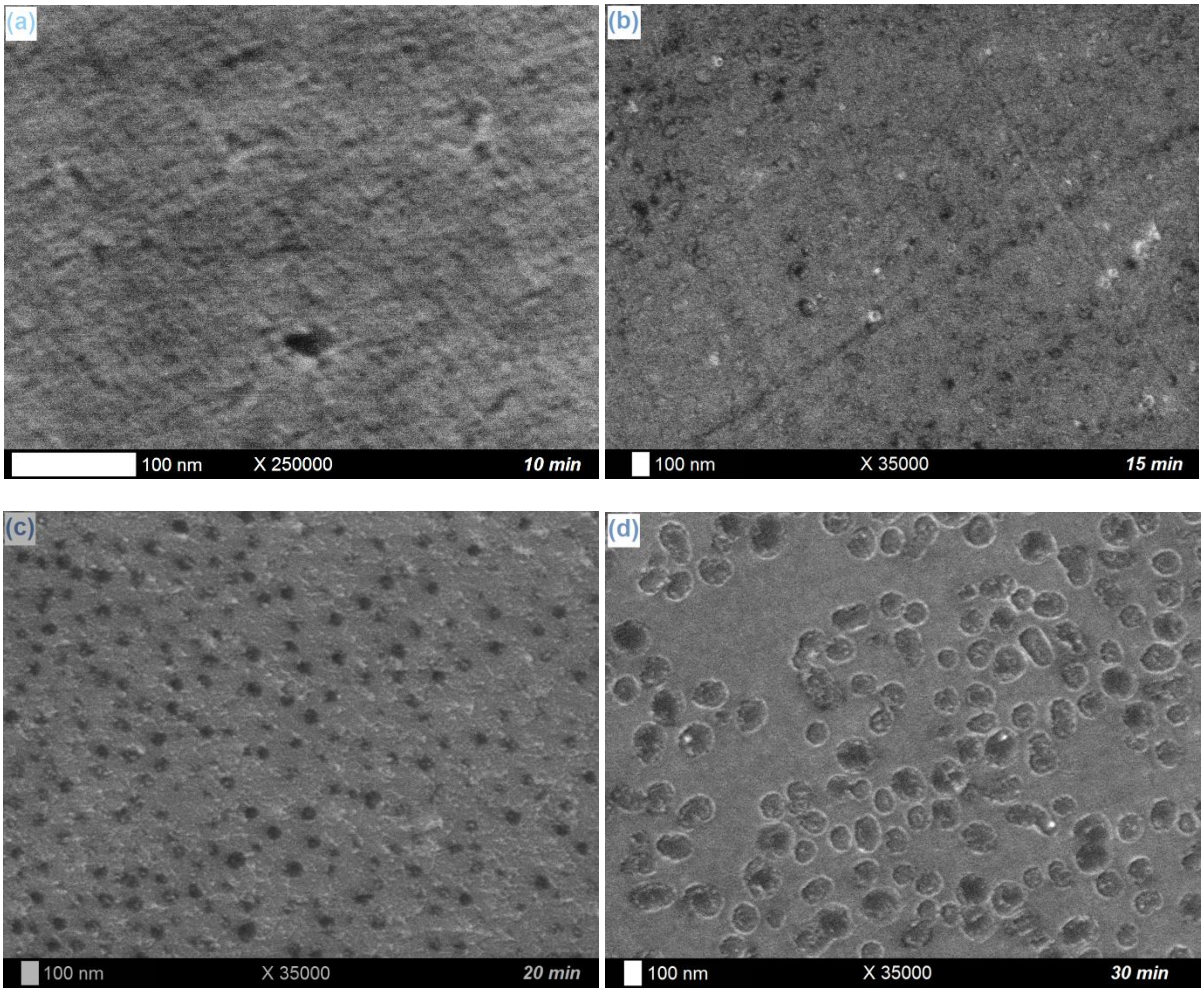
(a)
100 nm
X 250000
10 min
(b)
100 nm
X 35000
15 min
(c)
100 nm
X 35000
20 min
(d)
100 nm
X 35000
30 min

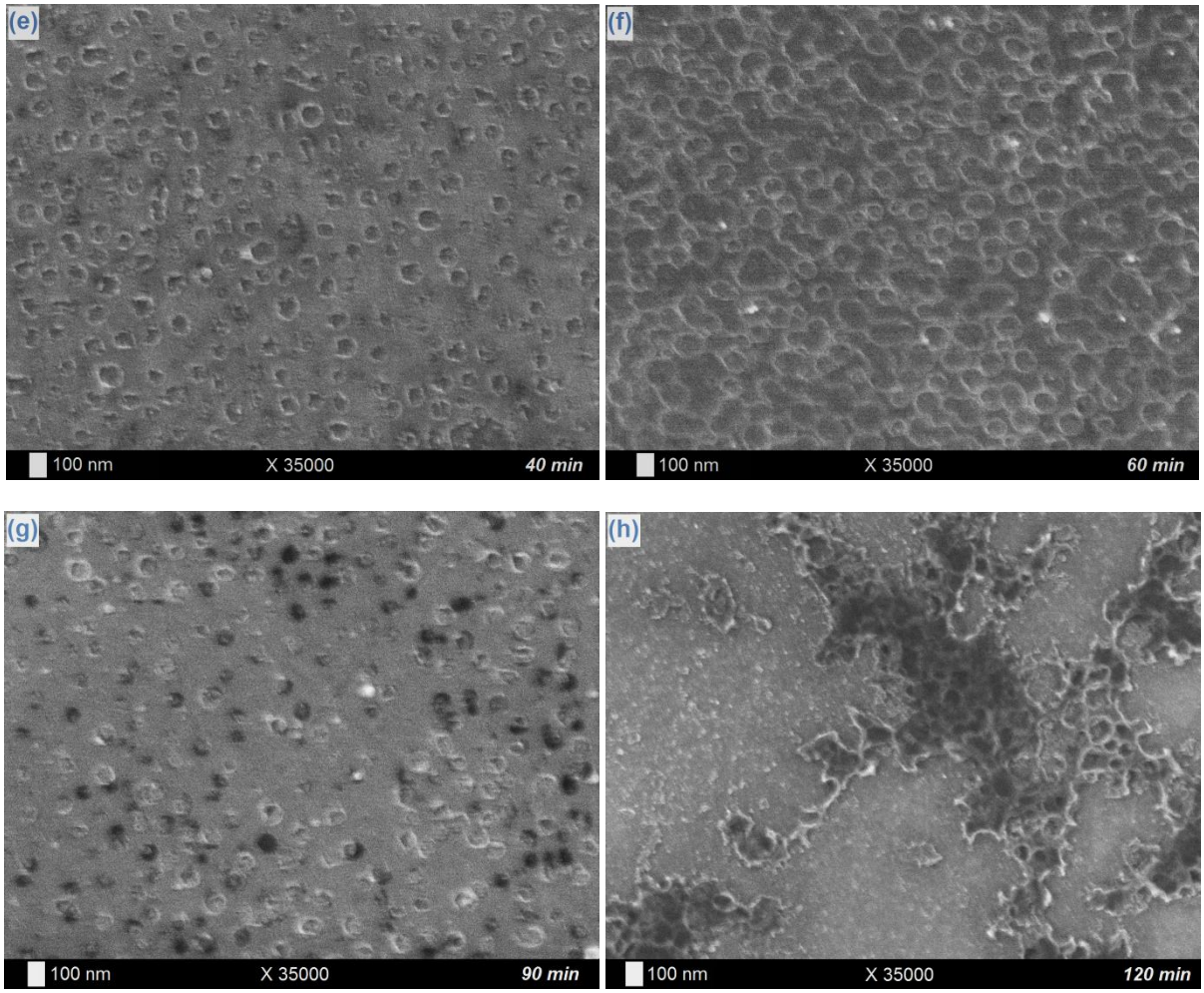

Fig. 8. SEM pictures of Ta layers galvanostatically electrodeposited on Nitinol plates at -100 µA/cm², 25°C and during 10 min (a), 15 min (b), 20 min (c), 30 min (d), 40 min (e), 60 min (f), 90 min (g), and 120 min (h).

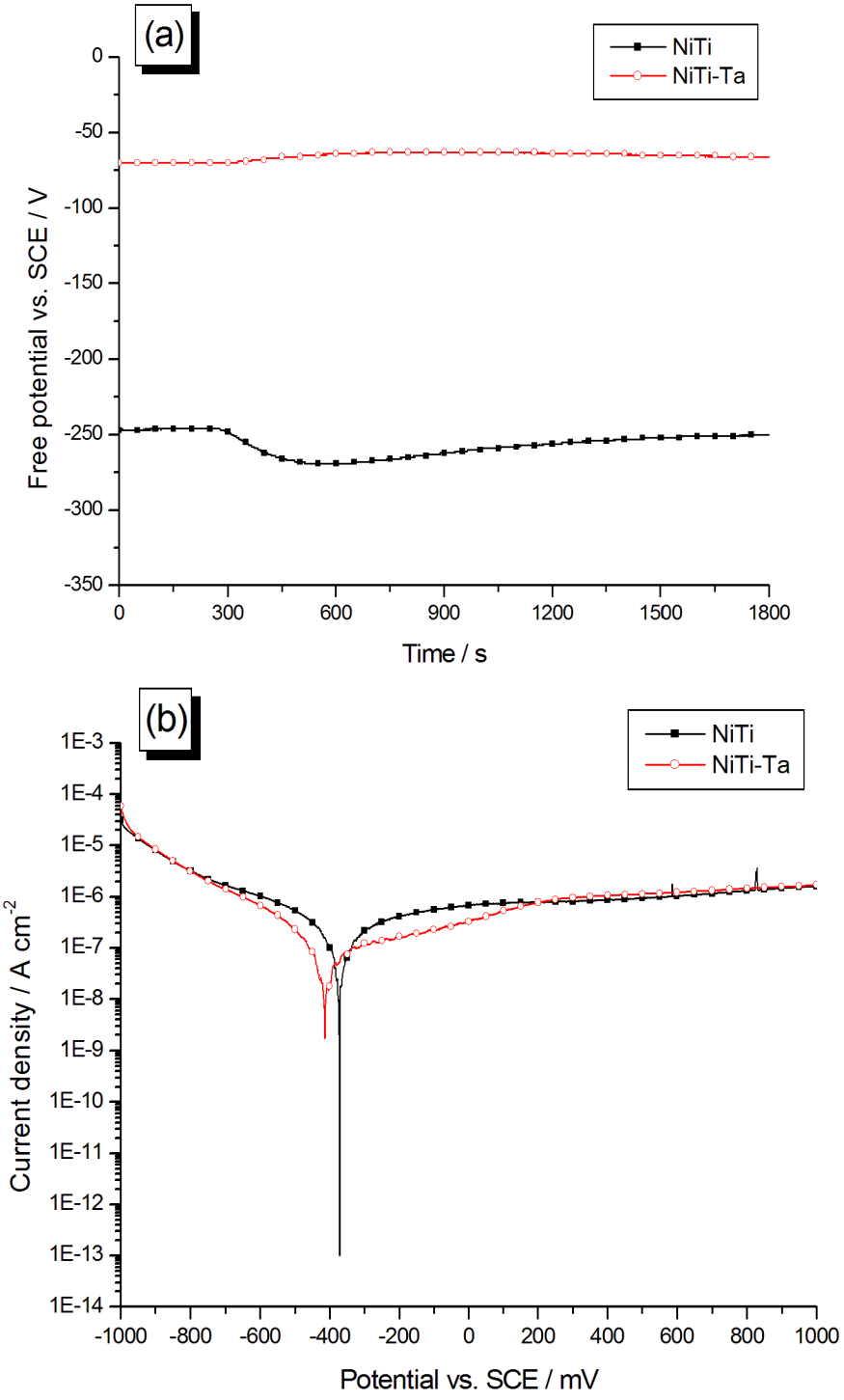

Fig. 9. Electrochemical characterizations of bare Nitinol (NiTi) and Nitinol covered with an electrodeposited Ta layer (NiTi-Ta). (a) Free potential measurements in NaCl 0.9%; (b) polarization curves in NaCl 0.9%, recorded at a scan rate of 1 mV/s.

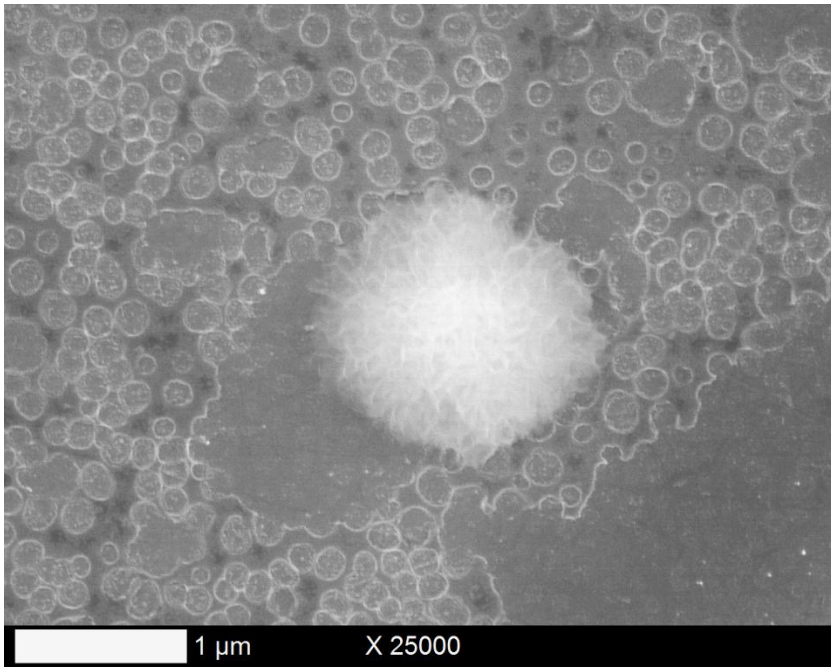

Fig. 10. SEM picture of an hydroxyapatite crystal deposited on a Ta-covered Nitinol plate.

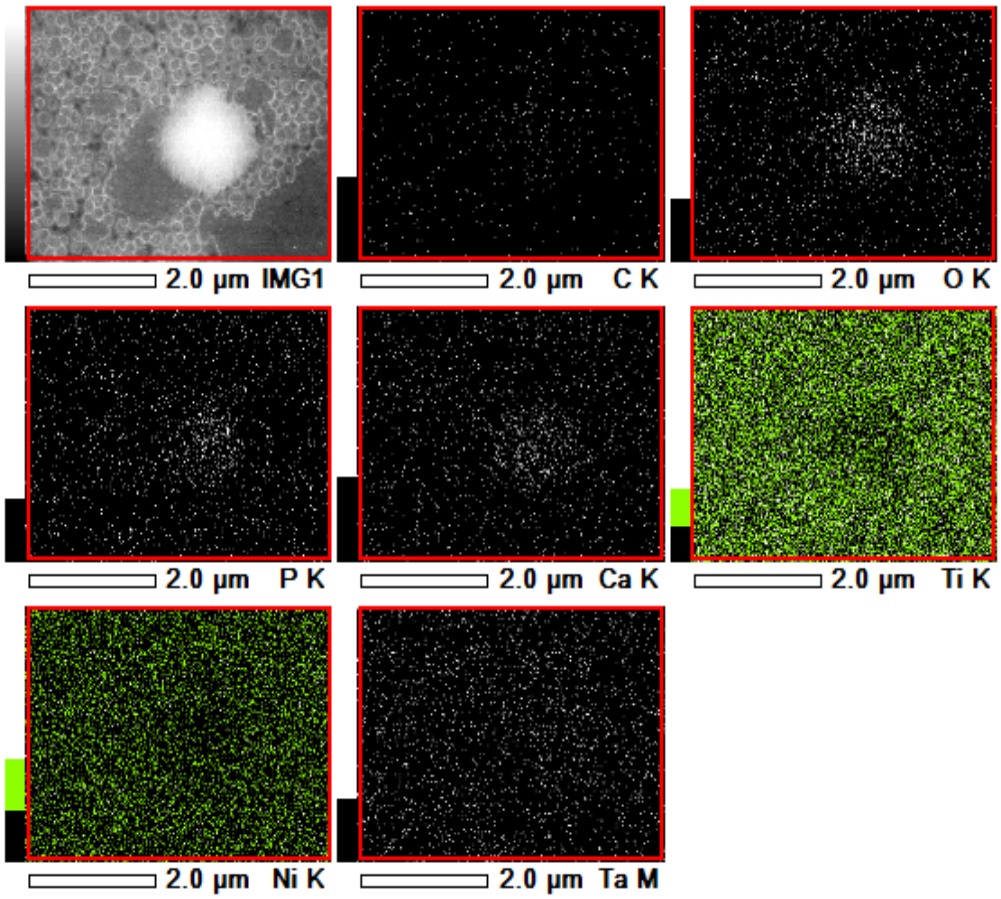

Fig. 11. EDX mapping (C K, O K, P K, Ca K, Ti K, Ni K and Ta M signals) of an hydroxyapatite crystal deposited on a Ta-covered Nitinol plate (SEM picture on Fig. 10).

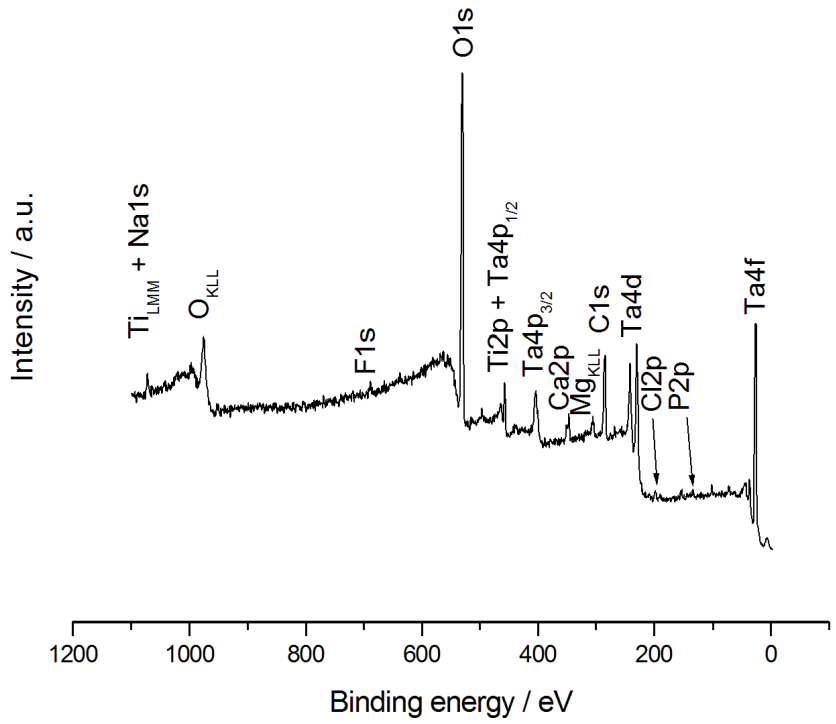

Fig. 12. XPS survey spectrum of an hydroxyapatite deposit generated on a Ta-covered Nitinol surface.

Figure captions

Fig. 1. Cyclic voltammogram of a Nitinol substrate in a 0.25 M LiF solution in [BMP]Tf_2N, with (plain line) and without (dash line) the presence of 0.10 M TaF_5. The curves are recorded at a scan rate of 100 mV/s and at room temperature (25°C).

Fig. 2a-c. SEM pictures of Ta layers galvanostatically electrodeposited on Nitinol at -100 µA/cm², 25°C and during 1 h.

Fig. 3. SEM picture of Ta layers electrodeposited on Nitinol plates, after peeling test.

Fig. 4. SEM pictures of Ta layers galvanostatically electrodeposited on titanium (a-b) and nickel (c-d) plates at -100 µA/cm², 25°C and during 1 h.

Fig. 5. XPS survey spectrum (a) and Ta4f (b), F1s (c), Ti2p (d), and Ni2p (e) core levels of a Nitinol substrate covered by a Ta electrodeposit.

Fig. 6. EDX mapping (red spots highlight Ta presence – Ta M signal) of one pore in the Ta layer covering a Nitinol substrate.

Fig. 7. SEM pictures of Nitinol surfaces after contact with a 0.25 M LiF / [BMP]Tf_2N solution during 1 h at 25°C (a-b) with an applied current density of -100µA/cm² and (c-d) in open circuit conditions (without current). Bare Nitinol surfaces are also presented for the sake of comparison (e).

Fig. 8. SEM pictures of Ta layers galvanostatically electrodeposited on Nitinol plates at -100 µA/cm², 25°C and during 10 min (a), 15 min (b), 20 min (c), 30 min (d), 40 min (e), 60 min (f), 90 min (g), and 120 min (h).

Fig. 9. Electrochemical characterizations of bare Nitinol (NiTi) and Nitinol covered with an electrodeposited Ta layer (NiTi-Ta). (a) Free potential measurements in NaCl 0.9%; (b) polarization curves in NaCl 0.9%, recorded at a scan rate of 1 mV/s.

Fig. 10. SEM picture of an hydroxyapatite crystal deposited on a Ta-covered Nitinol plate.

Fig. 11. EDX mapping (C K, O K, P K, Ca K, Ti K, Ni K and Ta M signals) of an hydroxyapatite crystal deposited on a Ta-covered Nitinol plate (SEM picture on Fig. 10).

Fig. 12. XPS survey spectrum of an hydroxyapatite deposit generated on a Ta-covered Nitinol surface.

Tables

Sample	Ni2p/Ti2p
Bare Nitinol	1.03
Nitinol 1 h in 0.25 M LiF / [BMP]Tf_2N	
With applied current density of -100 µA/cm²	0.43
Without applied current density	0.44

Table 1. XPS Ni2p/Ti2p ratios of Nitinol samples after pretreatment ("bare Nitinol") and after a 1 h contact with the fluorine working solution containing no TaF_5 precursor, with and without application of a -100 µA/cm² current density.

Sample	Ta4f/(Ni2p+Ti2p)	Ni2p/Ti2p	Ni2p/Ta4f
Bare Nitinol	--	1.03	--
Nitinol covered with Ta after an electrodeposition time of			
10 min	2.40	0.71	0.17
15 min	2.74	0.91	0.18
20 min	2.72	1.73	0.70
30 min	2.79	1.94	0.67
40 min	2.83	1.71	0.22
60 min	2.88	2.97	0.26
90 min	4.57	Only Ni is detected	0.28
120 min	Ni, Ti undetected	//	//

Table 2. XPS Ta4f/(Ni2p+Ti2p), Ni2p/Ti2p and Ni2p/Ta4f ratios of Nitinol samples after pretreatment ("bare Nitinol") and covered with a Ta layer after various electrodeposition durations.

Sample	E_{free} (mV/SCE)	E_{cor} (mV/SCE)	j_{cor} (10^{-8} A/cm²)
Bare Nitinol	-257	-355	15.2
Nitinol covered with Ta 1 h, -100 µA/cm²	-67	-529	2.34

Table 3. Free potential, corrosion potential and corrosion current density of bare and Ta-modified Nitinol substrates.